VOL. 16, NO. 18, SEPTEMBER 2021 ISSN 1819-6608
ARPN Journal of Engineering and Applied Sciences

www.arpnjournals.com

ENERGY SAVING IN RESONANT WIRELESS CHARGER USING SELF-OSCILLATING RESONANT INVERTER WITH P&O ALGORITHM

Ramón Álvarez-López, José López-Prado and José Araque-Gallardo
Department of Electronics Engineering, Faculty of Engineering, University of Sucre, Colombia
E-Mail: ramon.alvarez@unisucre.edu.co

ABSTRACT

The wireless charging of electronic devices, such as electric vehicles, is an alternative that promises comfort and convenience to the user. The resonant converters are an important alternative for the implementation of power conditioning circuits with an excellent density/power ratio, this backed by high efficiency and the possibility of switching the transistors to low currents and voltages. A limitation of the wireless charging systems of a resonant nature is the dependence between the parameters of the resonant filter and the power delivered to the load. In this work, a control alternative for a resonant DC-DC converter is presented. The simulation results validate the proposed hypothesis, in which the possibility of obtaining a DC-DC resonant converter operating at the maximum power predicted by the tank before variations in its parameters is manifested.

Keywords: resonant wireless charger; perturb and observe algorithm.

INTRODUCTION

The saving and efficient use of energy is a subject of great relevance at present. One of the most accepted forms of energy saving at an international level is the incorporation of power conditioning systems based on electronic systems, equipped at the same time with an energy management system that obeys a set of policies defined by users. The electronic power converters represent a particular case of power conditioning systems because they have become ubiquitous stages in energy management systems.

Electronic power conditioning systems increasingly use converters based on resonant inverters [1], such as seen in Figure-1. The above is motivated to a great extent because of the devices of the resonant inverter switch to low voltages and currents (soft switching), which implies lower losses due to switching [2]. The resonant inverter produces output voltages and currents in the form of a sine wave (for frequencies close to the resonance frequency) resulting from the resonance of a tank circuit, that is, formed by inductances and capacitors [3], [4]. Generally, the resonant inverter is used to couple in AC the different stages of a power conditioning system from a DC input [3], [5], [6]. The resonance frequency of a resonant inverter is conveniently selected to reduce the size of the circuit inductor or transformer, that is, high switching frequencies.

Recent publications have proposed self-excited resonant inverters that operate at the resonance frequency in the order of Megahertz [2], [7]–[10]. Said resonance frequency depends exclusively on the parameters of the tank circuit. This implies that small variations in the parameters of the circuit resulting in large frequency variations and consequently reduction of the output power. In this work, a proposal of a series DC-DC resonant converter is made as an alternative to solve the problem of variation of parameters of the tank circuit and the load [11]. Initially, an analysis is made of the proposed converter and the series resonant architecture used as a tank circuit. Then, a description and analysis of the controlled series resonant converter are made using a tracking algorithm of the maximum power point. Finally, the results obtained through simulations for the proposed converter are presented.

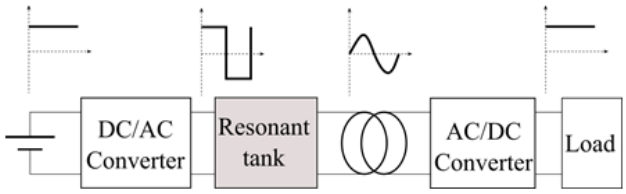

Figure-1. Block diagram of the resonant DC-DC converter.

SERIES RESONANT CONVERTER (SRC) ANALYSIS

Circuit Description

Figure-2 shows the typical circuit of a DC / DC converter that uses a series resonant inverter. As can be seen, the DC/AC converter consists of a MOSFET H-bridge inverter, meanwhile, the resonant circuit is an L-C tank, coupled with the AC/DC output converter through a transformer.

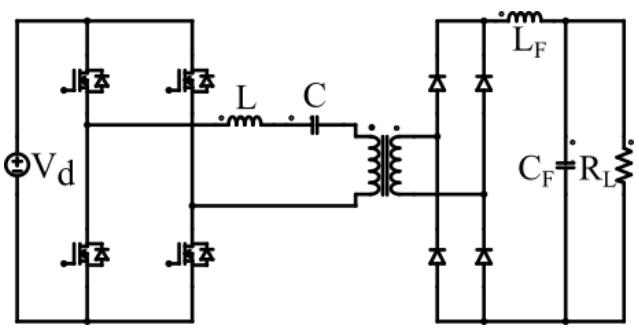

Figure-2. Series resonant converter.

Equivalent Circuit

A model based on the first harmonic approximation is used to obtaining an equivalent circuit to represent the effect of rectifier and load. Analysis of SRC is done using AC analysis method in which the equivalent the square wave input voltage and the equivalent AC resistance replace the inverter and output rectifier [12]. The equivalent circuit of SRC is given in Figure-3.

Figure-3 shows a series resonant inverter circuit with resistive loading. If the switching transients of the inverter are not of primary interest, the inverter output may be replaced with an equivalent source. Figure-3 shows a simple equivalent circuit representation of a system in which the transformer and load are represented by a referred RL impedance and the inverter output is represented by an equivalent square wave source. The system equation is given by the following KVL Eqn. (1).

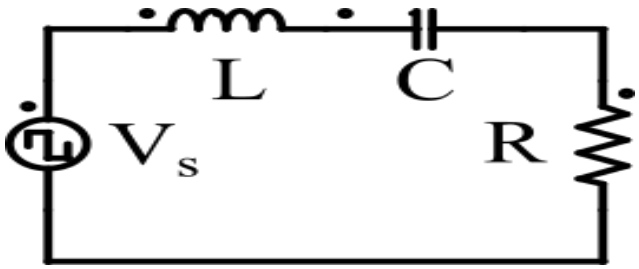

Figure-3. Equivalent SRC circuit.

$$v_L + v_R + v_C = v_S \quad (1)$$

Using:

$$i_L = C \cdot {dv_c}/{dt}, v_L = L \cdot {d^2}/{dt^2}. \text{and } v_R = R \cdot i_L$$

The system equation, expressed in terms of the capacitor voltage, v_c, is as shown in Eqn. (2):

$$\frac{d^2 v_C}{dt^2} + \frac{R}{L}\frac{dv_C}{dt} + \frac{v_C}{LC} = \frac{v_S}{LC} \quad (2)$$

For a response of that is under-damped, the roots of the characteristic equation of the above system equation are complex. Defining $2\alpha = {R}/{L}$ and the series resonant frequency, $\omega_0 = {1}/{\sqrt{LC}}$, the pair of complex roots may be written as Eqn. (3):

$$s_{1,2} = -\alpha \pm \sqrt{\alpha^2 - \omega_0^2} \quad (3)$$

From which we see that the damped resonant frequency is:

$$\omega_d = \sqrt{\alpha^2 - \omega_0} \quad (4)$$

The admittance of the series RLC branch at the frequency is given by Eqn. (5):

$$Y(jw) = \frac{1}{jwL+R+1/jwC} = \frac{1}{R}\frac{2\alpha(jw)}{(jw)^2+2\alpha(jw)+\omega_0^2} \quad (5)$$

In terms of the quality factor, Q, defined as ${\omega_0}/{\alpha}$, we can write the Eqn. (5) as Eqn. (6):

$$Y(jw) = \frac{1}{R}\frac{(1/Q)(jw/w_0)}{(jw/w_0)^2+(1/Q)(jw/w_0)+1} \quad (6)$$

Using circuit elements with a higher Q value will result in a sharper or more selective $Y(j\omega)$ characteristic, but then the peak voltage across the capacitor which is equal to Q times the source voltage at resonance will be correspondingly higher.

Let's now consider a circuit proposed in [12] where $R = 12\Omega$, $L = 231mH$, $C = 0.1082251\mu F$, and V_{DC} has a value of 100 volts. Since the power delivered to the load resistor, *R*, is *2R*, the current, *i*, is controlled by varying the frequency of the square wave inverter output.

The fundamental component of the square wave voltage of magnitude V_{DC} has a peak value of $4V_{DC}/\pi$, or a RMS value of $4V_{DC}/\pi\sqrt{2}$. For the given values of *RLC* and V_{DC}, a maximum power of 675.47 W is deliverable to *R* at the resonant frequency of 200x10^3 rad/sec. Figure-4 shows the plots of the admittance of the series *RLC* circuit at the power deliverable to R with the fixed dc voltage close to its resonant frequency.

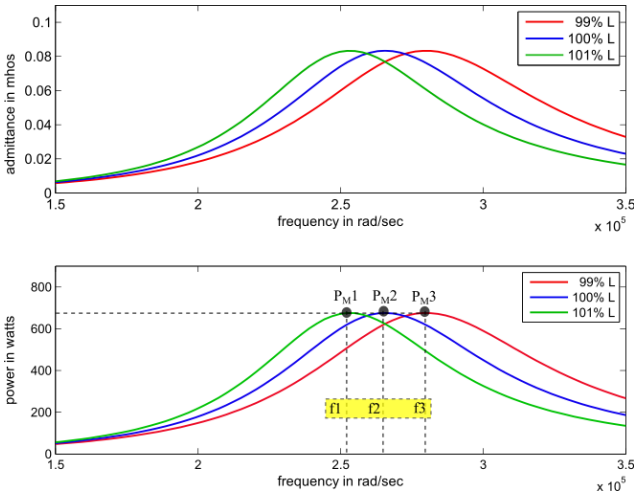

Figure-4. Admittance of the series RLC circuit at the power deliverable to R with the fixed dc voltage close to its resonant frequency.

POWER CLOSED-LOOP CONTROL DESIGN BASED ON PERTURB AND OBSERVE (P&O) ALGORITHM

Block Diagram of the Proposed Control System

Figure-5 describes the blocks of the series resonant converter with maximum power point tracking or MPPT. The square wave inverter operates as a voltage controlled power oscillator (VCO), where the output frequency is a function of the input voltage derived from the block of maximum power point tracking, this

is $f_S(v[k])$. The function of the MPPT algorithm is to ensure that the converter operates at the resonant frequency regardless of variations in circuit parameters. The MPPT is developed through the implementation of the technique of perturb the input voltage to the VCO and observe the variation of power. The control block based on the P&O algorithm takes advantage of the current measurement in the SRC output network to recalculate the voltage reference that must be provided to the VCO.

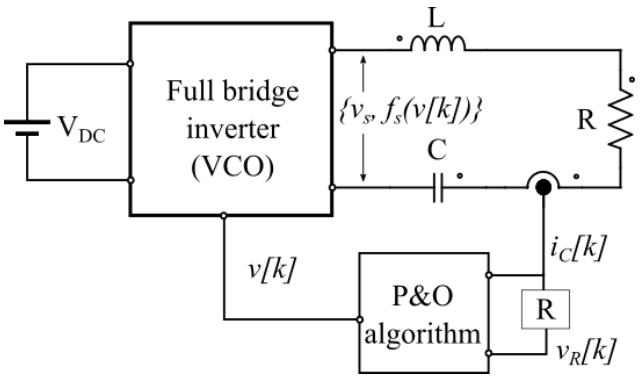

Figure-5. Block diagram of the proposed control system.

Perturb and Observe Algorithm (P&O)

The logic of the P&O algorithm and the flowchart are explained in Figure-6 [11]. The operating voltage of the VCO is perturbed by a small increment of *K* and this resulting change in frequency and output power. If the power changing is positive, the perturbation of the operating voltage (operating frequency) needs to be in the same direction as the increment. On the contrary, if the power changing is negative, the obtained system operating point moves away from the MPPT and the operating frequency needs to move in the opposite direction of the increment. When the MPPT is reached, the output power of converter oscillates around the maximum.

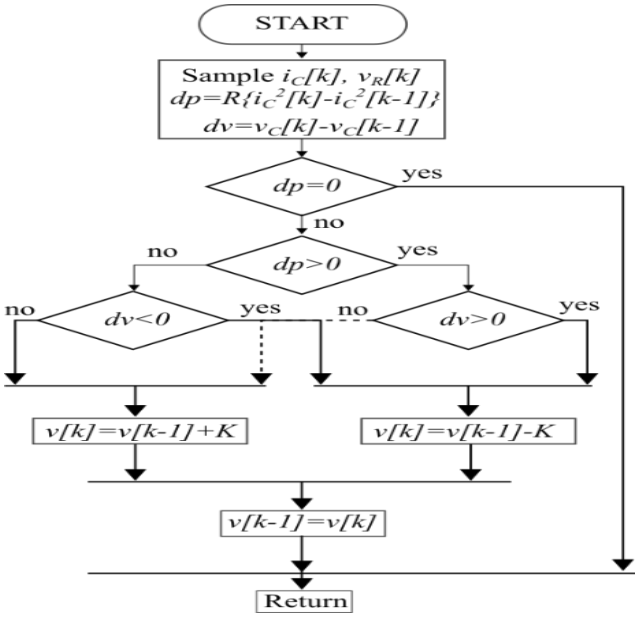

Figure-6. The logic of the P&O algorithm and flowchart.

SIMIULATION RESULTS

Figure-7 describes the block diagram used to simulate the proposed control scheme. The simulations have been developed in Matlab-Simulink, following the methodology of the first harmonic analysis, which is guaranteed by the implementation of low-pass filters [12]. It can be seen that the square wave inverter bridge has been implemented as a power VCO, where the angular frequency is calculated by a proportional-integral block from the voltage setpoint provided by the P&O block.

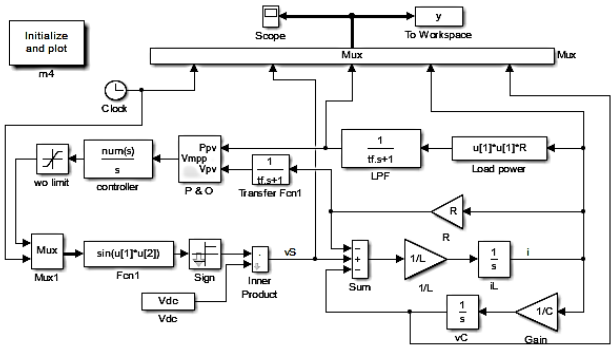

Figure-7. The logic of the P & O algorithm and flowchart.

Figure-8 and Figure-9 presents the simulation results obtained for the evaluation of the proposed control scheme for the *SRC*. Figure-8 shows the time evolution of the output power. We can see the influence of the P&O algorithm on the output power (*Pout* compensated). It is noted that said compensation allows extracting the maximum power from the *SRC*. On the other hand, Figure-9 shows the time evolution of the used signal as a frequency reference, which is calculated by the P&O algorithm in each time evolution of the use signal as a frequency reference control cycle. It can be seen that for the given system, the frequency setpoint is updated to force the *SRC* to deliver its maximum power.

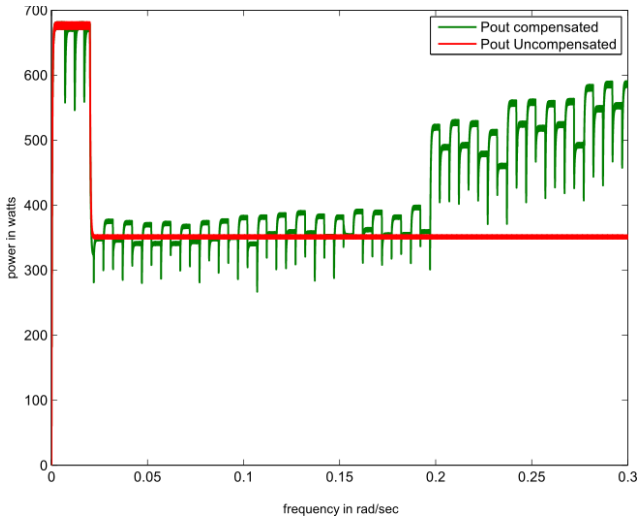

Figure-8. Time evolution of the output power.

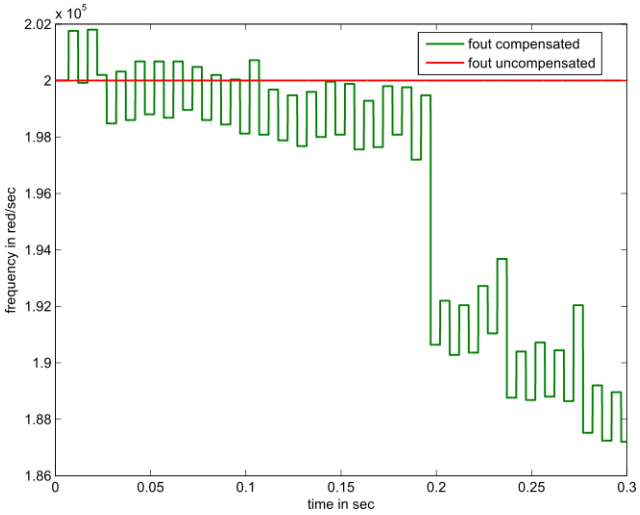

Figure-9. Time evolution of the used signal as a frequency reference.

CONCLUSIONS

The simulation results allow the control system to also provide the development of a self-excited DC-DC converter. Operating at maximum power allows compensating leakage losses typical of a resonant converter.

The MPPT algorithm uses only one current sensor, from which the power trend can be inferred, which facilitates the implementation of the proposed converter. In the case of operating with non-resistive loads, it is essential to measure the output voltage of the converter.

The proposed converter tends to operate at low frequencies during the start transient, so a technique must be implemented to mitigate the negative effects that this may cause for the load.

ACKNOWLEDGMENT

We appreciate the support of the program "EcosistemaCientífico- Proyecto Cod 58667"- Strategy of the transformation of the Colombian energy sector in the Horizon 2030, and the support of GINELECT University of Sucre Research Group.

REFERENCES

[1] M. Arazi, A. Payman, M. B. Camara and B. Dakyo. 2018. Study of different topologies of DC-DC resonant converters for renewable energy applications. 2018 13th Int. Conf. Ecol. Veh. Renew. Energies, EVER, 2018. pp. 1-6.

[2] C. Lorenzini, J. V. Flores, L. F. A. Pereira and L. A. Pereira. 2018. Resonant–repetitive controller with phase correction applied to uninterruptible power supplies. Control Eng. Pract. 77(October 2017): 118-126.

[3] P. J. Baxandall. 1959. Transistor sine-wave LC oscillators. Some general considerations and new developments. Proc. IEE - Part B Electron. Commun. Eng. 106(16S): 748-758.

[4] S. D. Johnson, A. F. Witulski and R. W. Erickson. 1988. Comparison of resonant topologies in high-voltage DC applications. IEEE Trans. Aerosp. Electron. Syst. 24(3): 263-274.

[5] H. Jafarzadeh, A. Sahab and A. G. Pastaki. 2018. DC-DC converter series resonant nonlinear optimal control using GBM and firefly algorithm. 2017 IEEE Int. Conf. Cybern. Comput. Intell. Cybern. 2017 - Proc. 2017-Novem: 1-5.

[6] R. Bonache-Samaniego, C. Olalla and L. Martinez-Salamero. 2017. Dynamic modeling and control of self-oscillating parallel resonant converters based on a variable structure systems approach. IEEE Trans. Power Electron. 32(2): 1469-1480.

[7] N. Madhanakkumar, T. S. Sivakumaran, D. Sujitha and A. L. L. C. R. Converter. 2014. Comparison Analysis of PI and Fuzzy Control of LLC Resonant Converter Incorporating ZVS Boost Converter. pp. 20-26.

[8] E. Reyes-Moraga, A. Watson, J. Clare and P. Wheeler. 2013. Predictive control of a direct resonant converter with output voltage compensation for high voltage DC power supply applications. 2013 15th Eur. Conf. Power Electron. Appl. EPE 2013.

[9] L. J. Liu *et al*. 2016. Analysis on voltage oscillation of a mid-frequency series resonant inverter for DRMP coils on J-TEXT. Fusion Eng. Des. 102: 59-65.

[10] J. L. Portal, F. E. López, M. Morera, L. León and A. Amador. 2010. Estudio del empleo de inversores resonantes de alta frecuencia en la recuperación de fuentes de soldadura. (Spanish). Rev. Ing. Energ. 31(1): 3-9.

[11] A. Jeyalakshmi and M. Prabhakar. 2006. Effect of leakage inductance on the performance of parallel resonant converter. Int. Symp. Power Electron. Electr. Drives, Autom. Motion, 2006. SPEEDAM 2006. pp. 1338-1341.

[12] O. Chee-Mun. 1998. Dynamic simulation of electric machinery using MATLAB/SIMULINK. Prentice Hall PTR.